This is the author's version of an article that has been published in this journal. Changes were made to this version by the publisher prior to publication.
The final version of record is available at http://dx.doi.org/10.1109/TCSII.2015.2482578

A New 2^{nd}–Order Allpass Filter in 130nm CMOS

Peyman Ahmadi*, Brent Maundy*, A. S. Elwakil** , Leonid Belostotski*, and Arjuna Madanayake***

* Department of Electrical and Computer Engineering, University of Calgary, Calgary, Alberta, Canada, T2N1N4

** Dept. of Electrical & Computer Engineering, University of Sharjah, Emirates (email: elwakil@ieee.org).

*** Department of Electrical and Computer Engineering, University of Akron, Akron, Ohio, USA, 44325-3904.

***Abstract*—This paper presents a novel wide-bandwidth second order voltage mode allpass filter derived from a canonical single transistor bandpass filter. The core of the circuit consists of only one transistor, two resistors and two energy storage elements. The operation of the proposed filter is validated experimentally. A filter implemented in IBM 0.13 μm CMOS was measured to have 55 ps group delay across 6 GHz bandwidth while consuming 18.5 mW from a 1.5-V supply. This work experimentally demonstrates a CMOS allpass filter that operates at multi-GHz frequencies and achieves the highest delay-bandwidth product (DBW) compared to previously published CMOS allpass filters known to the authors.**

***Index Terms*—Keywords: Active filters, Analog circuits, Filter theory, All-pass filters, Q factor.**

I. Introduction

ALLPASS filters have wide application in electronic circuits [1]. Generally, they are used for linear phase shifting, while keeping the signal amplitudes constant over the desirable frequency range. They can also be used to implement high-quality-factor frequency-selective filters and to realize biquadratic filters to synthesize quadrature and multiphase oscillators [2]–[4]. In addition, allpass filters are key components in the realization of time delays that find applications in differential modulation [5], transmit-reference systems [6], beamforming [7]–[9], and impulse radio ultra-wideband wireless receivers for synchronizing the received RF signal with the locally generated pulse signal [10], to name a few examples. Allpass filters have also been finding applications in circuits that conventionally relied on digital delay stages. The conventional implementation of such circuits relies on analog-to-digital converters (ADCs) for digitizing the signals, which are subsequently passed through a digital FIR filter-based delay circuit. Such circuits suffer from clock injection issues, temporal aliasing, quantization noise, and are limited by the ADC bandwidth. Using analog techniques removes these issues but still permits the implementation of such circuits with continuous time delay stages implemented with allpass filters, albeit with higher noise and linearity problems [7], [8]. This work focuses on replacing the traditional digital delay stages such as those used in [8] and illustrated in Fig. 1 with wideband analog delay stages.

To realize true time delays there are several well known approaches, such as using transmission lines [10], lumped LC delay lines [11], or active devices [12], [13]. Transmission lines and LC delay lines are area-inefficient and experience losses when cascaded. They may also consume significant amounts of power due to their low impedance. Active circuits therefore, are more flexible in terms of integration, even though their achievable delay is limited [12], [13]. Alternatively, approximations such as the Bessel-Thomson or Padé approximation or a cascade of infinite order allpass sections can be used to approximate a

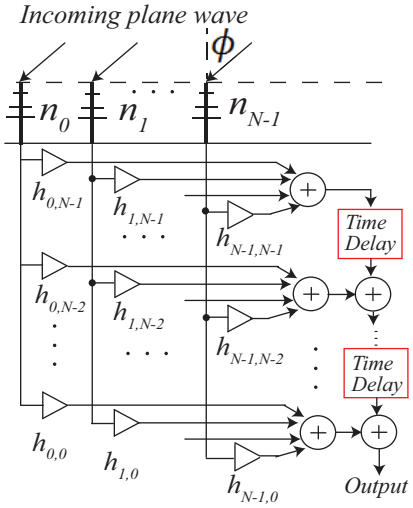

Figure 1. An example of employing time delays in an FIR-based beamformer with N antennas in the array. The beamformer coefficients are shown as h's and explained in [8].

true time delay of e^{-sT}, $s \in C$. For the infinite-order allpass approximation, a cascade of $M \in \mathbb{Z}^+$ allpass filters yields

$$e^{-sT} = \left(\frac{e^{\frac{-sT}{2M}}}{e^{\frac{sT}{2M}}} \right)^M = \left(\frac{1 - \frac{sT}{2M} + \frac{1}{2}\left(\frac{sT}{2M}\right)^2 - \ldots}{1 + \frac{sT}{2M} + \frac{1}{2}\left(\frac{sT}{2M}\right)^2 + \ldots} \right)^M \quad (1)$$

If the infinite order polynomials in the numerator and denominator of (1) are approximated to order two, then $e^{-sT} \approx \frac{1-\frac{sT}{2M}+\frac{s^2T^2}{8M^2}}{1+\frac{sT}{2M}+\frac{s^2T^2}{8M^2}}$ represents the well known second-order allpass filter.

Several current- and voltage-mode allpass filters can be found in the literature [14]–[19]. Most of these filters use one or more operational voltage or current amplifiers [20] to realize circuits, such as four terminal floating nullors (FTFN), Second Generation Current Conveyors (CCIIs), voltage-differencing inverting buffered amplifiers (VDIBA) and current difference buffered amplifiers (CDBA) [14], [16], [17], [19]. The bandwidths of these circuits however, are significantly decreased by the parasitic capacitance at their high impedance nodes limiting the application domain of the filters to low frequencies. Furthermore, there are only a few voltage-mode allpass filters in the literature, which can operate at radio frequencies (RF) [6], [8], [9], [12], [21].

In the work of [22], single transistor active filters were first explored based on six general voltage-input, voltage-output transfer functions, surrounded by the minimum number of passive elements (two resistors and two energy storage elements). All the results for valid second order filters of the lowpass, highpass, bandpass and bandstop variety filters were tabulated and verified.

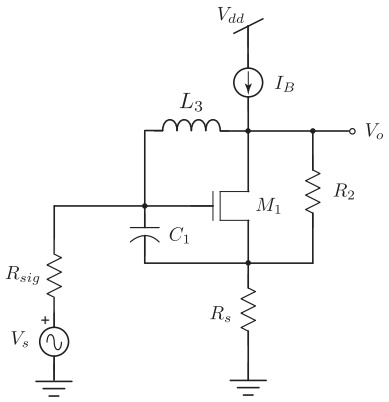

Figure 2. A canonical allpass filter derived from its equivalent bandpass filter taken from Table IV, Type 1, Filter #1 of [22].

It is well known however, that allpass filters derived from bandpass filters by using the complimentary theorem possess excellent tracking characteristics because the zero frequency tracks the pole frequency[1]. In [22] this occurs when constant $K = 2$ and hence several such allpass filters are possible from Tables II-IV in [22]. Note that not all the allpass filters derived using the complementary theorem can be easily biased to ensure transistors operate in their desired operating region nor can K always be set equal to 2. One example being a Table IV, Type-1(filter #2) which cannot be properly biased because at DC (assuming a MOSFET transistor is used as the active device), L_1 shorts the gate and source nodes resulting in $V_{gs} = 0$. Likewise, the Table II, Type-3 (filter#13) while easy to bias, attempting to set $K = 2$ results in g_m being negative which is not possible. One attractive canonical LC allpass filter which is easily biased and K can be easily set to 2, is obtained from a Table IV, Type-1 (filter #1) topology and is presented in this paper and its performance evaluated. This circuit, its nonidealities and therefore its performance is the focus of this paper for possible use in high frequency beamforming applications.

This paper is therefore divided as follows: Section II looks at the allpass filter derived from the basic bandpass filter. Next non-ideal effects in the circuits are considered in Section III. Experimental and simulated results are presented in Section IV. Finally, we present our conclusions in Section V.

II. Proposed Allpass Filter

Consider the circuit shown in Fig. 2 derived from Table IV, Type-1, Filter #1 of [22] using the complementary theorem with $Z_1 = 1/sC_1$, $Z_2 = R_2$ and $Z_3 = sL_3$. Current source I_B determines the g_m of MOSFET M_1 and provides tunability for calibration purposes. Neglecting the intrinsic parasitic capacitances and the generator internal resistance R_{sig} for the moment, the ideal circuit transfer function of this circuit is easily computed as

$$H_2(s) = \frac{s^2 + (1-K)\frac{\omega_z}{Q}s + \omega_z^2}{s^2 + \frac{\omega_o}{Q}s + \omega_o^2} \tag{2}$$

[1]Worth mentioning is the fact that each of the six voltage-input, voltage-output transfer functions of [22], and by extension allpass filters derived from bandpass filters can be converted into current-input, current-output filters using the adjoint network theorem if their adjoint network exists.

where

$$K = \frac{1 + g_m R_2}{1 + \frac{R_s R_2 C_1}{L_3}} \tag{3a}$$

$$\omega_o = \omega_z = \sqrt{\frac{1 + \frac{R_2}{R_s} + g_m R_2}{C_1 L_3}} \tag{3b}$$

$$Q = \frac{\sqrt{C_1 L_3 \left(1 + \frac{R_2}{R_s} + g_m R_2\right)}}{C_1 R_2 + \frac{L_3}{R_s}} \tag{3c}$$

and the DC gain of this circuit is 1. The value of g_m that results in $K = 2$ which yields an allpass transfer function is therefore given by

$$g_m = \frac{1}{R_2} + \frac{2C_1 R_s}{L_3} \tag{4}$$

which results in pole (and zero) frequency

$$\omega_o = \omega_z = \sqrt{\frac{1}{C_1 L_3}\left(2 + \frac{R_2}{R_s} + \frac{2C_1 R_2 R_s}{L_3}\right)} \tag{5}$$

and pole/zero quality factor

$$Q = |Q_z| = \frac{\sqrt{2R_2 R_s + \frac{L_3}{C_1}\left(2 + \frac{R_2}{R_s}\right)}}{R_2 + \frac{L_3}{R_s C_1}}. \tag{6}$$

Note that because g_m appears in both (3b) and (3c) orthogonal tuning of this allpass filter is not possible unlike the second order allpass circuit of [13]. Also worth mentioning is the effective drain-source resistance the transistor sees is actually $R_2 /\!\!/ (1/g_{ds})$ but for $g_m \gg g_{ds}$ and $R_2 \ll (1/g_{ds})$, $R_2 /\!\!/ (1/g_{ds}) \cong R_2$. Using (3c) and (4) it can be easily shown that to generate complex poles $(Q > 1/2)$ and zeroes of this filter, requires that

$$R_2 < 4R_s + \frac{L_3}{R_s C_1} + 4\sqrt{\left(R_s^2 + \frac{L_3}{C_1}\right)} \tag{7}$$

Conversely, if R_2 is chosen larger than the right hand side of the inequality of (7), $Q < 1/2$, resulting in two real poles and two real zeroes. Note for the special case of $R_2 = \infty$, with $g_m = \frac{2C_1 R_s}{L_3}$ a first order allpass transfer function of the form

$$H_1(s) = -\left(\frac{s - \frac{R_s g_m + 1}{R_s C_1}}{s + \frac{R_s g_m + 1}{R_s C_1}}\right) \tag{8}$$

results for this filter. In actual practice, with R_2 omitted completely, the output impedance $1/g_{ds}$ fills the role of R_2, such that (4) must be modified to $g_m = g_{ds} + 2C_1 R_s/L_3$ and real poles and zeroes will exist. This is because $1/g_{ds}$ will typically be greater than the right hand side of the inequality of (7), resulting in $Q < 1/2$.

Finally, the phase $\phi(\omega)$, group delay $\tau_g(\omega)$ and input impedance of the 2^{nd} order allpass filter $(R_2 < \infty)$ are given by

$$\phi(\omega) = -2\tan^{-1}\left[\frac{\omega L_3 (C_1 R_2 R_s + L_3)}{\omega^2 C_1 R_s L_3^2 - (R_2 + 2R_s) L_3 - 2C_1 R_2 R_s^2}\right] \tag{9}$$

$$\tau_g(\omega) = \tau_{g_o} \times \frac{\left(\omega^2/\omega_o^2 + 1\right)}{\left(\omega^2/\omega_o^2 - 1\right)^2 + \frac{\tau_{g_o}^2 \omega^2}{4}} \tag{10}$$

and

$$Z_{in}(s) = R_s \frac{s^2 + \left(\frac{R_2}{L_3} + \frac{1}{L_3 C_1}\right) s + \frac{2R_2R_s}{L_3^2} + \frac{1}{C_1 L_3}\left(2 + \frac{R_2}{R_s}\right)}{s^2 + \left(\frac{R_2}{L_3}\right) s + \frac{2R_2R_s}{L_3^2} + \frac{2}{C_1 L_3}} \tag{11}$$

respectively, where $\tau_{g_o} = \frac{2(C_1R_2R_s+L_3)}{R_2+2R_s+2C_1R_2R_s^2/L_3}$ is the delay at DC. Examining the input impedance expression of (11) we note that at low frequencies it has a value of $Z_{in} \cong R_s + 1/(2C_1R_s/L_3 + 2/R_2) \approx R_s + L_3/(2C_1R_s)$ for $C_1R_s/L_3 \gg 1/R_2$ which gradually reduces to R_s at high frequencies. In so far as the output impedance is concerned, assuming the circuit has a stimulus R_{sig}, then straightforward analysis shows that circuit has an output impedance of $Z_{out} = R_{sig} /\!\!/ \left((\frac{1}{g_m} /\!\!/ R_2) + R_s\right) \approx R_{sig} /\!\!/ (\frac{1}{g_m} + R_s)$ at low frequencies. Conversely the circuit has a value of $Z_{out} \cong R_2 + (R_s /\!\!/ R_{sig})$ at very high frequencies where C_1 shorts the gate and source of M_1 and L_3 acts as an open circuit. Note if R_{sig} is not negligible this would affect the filter's DC gain and the location of the pole frequency.

III. Non-Ideal effects

At RF frequencies it is well known that many high frequency effects affect the performance of every circuit. Most notably parasitic capacitances of which there are many giving rise to parasitic poles and zeroes. Considering the more common gate-source and gate-drain parasitic capacitances C_{gs} and C_{gd}, respectively it can be shown first that C_{gs} is in parallel with C_1 and therefore can be absorbed into C_1 for equations (3b)-(11). That is C_1^{new} replaces C_1 where, $C_1^{new} = C_1 + C_{gs}$, appropriately. Conversely, C_{gd} which appears in parallel with L_3 has an effect on the output resistance. At very high frequencies, C_{gd} shorts the drain and gate of M_1 and lowers the output resistance to $R_{sig} /\!\!/ R_s$. It also has the effect of adding an extra real zero and pole to the transfer function of (2) resulting in the transfer function being third order. To a first order approximation it can be shown that the additional single zero and single pole that arises because of the shunt C_{gd} is given by

$$\omega_{z_1} \approx \omega_{p_1} \approx -\frac{1}{R_2\left(C_1 + C_{gd}\right)} - \frac{1}{C_1}\left(\frac{1}{R_s} + g_m\right) \tag{12}$$

for $C_{gd} \ll C_1$. The corresponding new zero and new pole frequency is

$$\omega_z^{new} \approx \omega_o^{new} \approx \frac{1}{\sqrt{L_3\left(\frac{C_1}{1+\frac{R_2}{R_s}+g_mR_2} + C_{gd}\right)}} \tag{13}$$

Note that C_{gd} decreases the zero (and pole) frequency according to (13) when compared to (3b). In actual practice as C_{gd} increases relative to C_1, the zero frequency decreases but the pole frequency increases for g_m given by (4). Likewise the effect of the unwanted C_{gd} is to increase Q (and $|Q_z|$) and $\tau_g(\omega)$ above (3c) and (10), respectively subject to $Q < |Q_z^{new}| < Q^{new}$ with $\omega_z^{new} < \omega_o < \omega_o^{new}$, $\omega_{p_1} < \omega_{z_1}$ and $\tau_g^{new}(\omega) > \tau_g(\omega)$. Additionally, the single zero and single pole adds to the increased group delay $\tau_g^{new}(\omega)$ in the amount of $\approx \frac{(\omega_{p_1}+\omega_{z_1})(\omega^2+\omega_{p_1}\omega_{z_1})}{(\omega^2+\omega_{z_1}^2)(\omega^2+\omega_{p_1}^2)}$. In summary, the exact pole and zero locations must however, be determined in the final analysis by simulation and g_m adjusted accordingly to ensure the closest match in pole and zero frequencies for a desired group delay.

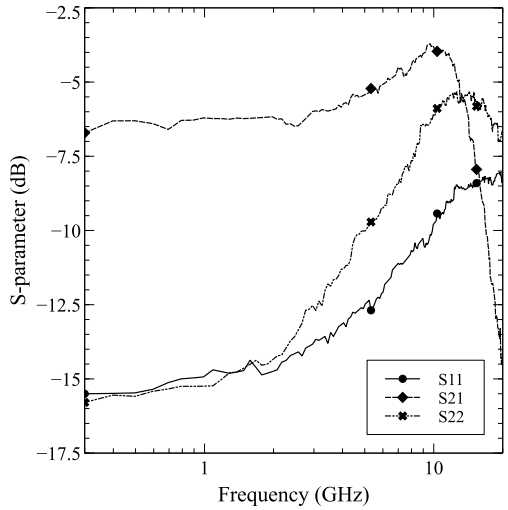

Figure 3. Measured S-parameters of the implemented allpass filter.

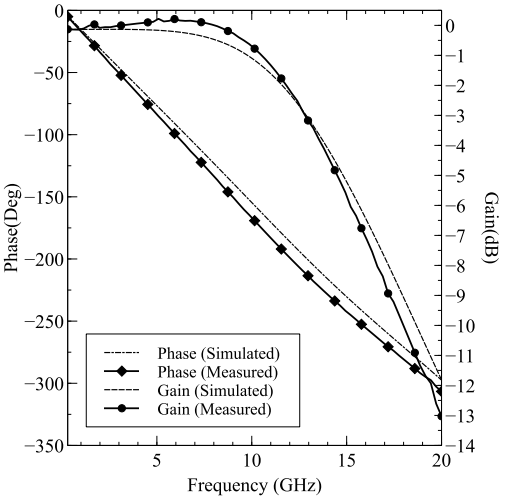

Figure 4. Phase and magnitude measured and simulated results of the proposed second order allpass filter. The simulated results are shown using dashed lines and experimental results using solid lines.

IV. Experimental and Simulated Results

To verify the functionality the second-order allpass filter was fabricated in IBM's $0.13\mu m$ CMOS technology. The filter was designed to operate to 6 GHz with $R_s = 30\Omega$, $R_2 = 650\Omega$, $L_3 = 2.2nH$, $C_1 = 2.25pF$ and $g_m = 62mA/V$ with a $Q = 0.36$. This produces an ideal delay of $49ps$ at low frequencies. The circuit was wafer probed and its S-parameters were measured and are shown in Fig. 3. The S-parameters were used to determine the frequency response of the voltage-mode filter. In Fig. 4 the measured (solid lines) and simulated (dashed lines), amplitude and phase responses are shown. The first thing to be observed is that the DC gain is slightly less than unity. This slightly less than unity gain was due in part to the circuit output impedance being less than simulated. The delay of the circuit was also measured and is shown in Fig. 5 compared to the extracted simulated result[2]. The difference in the measured

[2]While the group delay of the circuit in (10) depends on g_m, which is process, voltage and temperature dependent, the simulations do not show significant variations in group delay response. The group delay variation of the circuit was 2.4% from 100 Monte Carlo simulations.

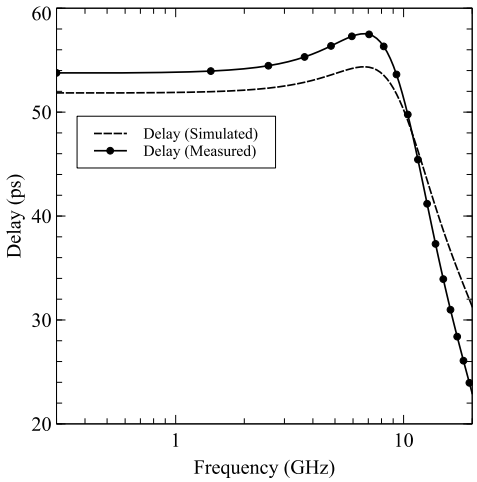

Figure 5. Measured versus simulated group delay of the allpass filter with frequency.

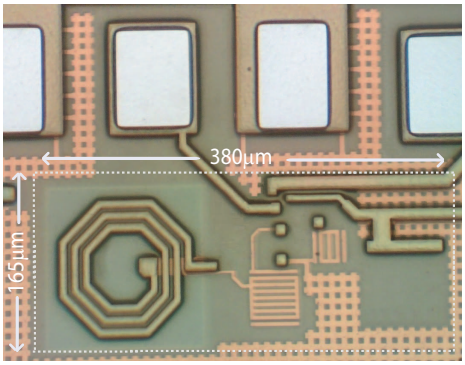

Figure 6. Microphotograph of the allpass filter which occupies an area of $380\,\mu m \times 165\,\mu m$.

versus experimental results was due to the parasitic capacitances, which create extra parasitic poles/zeroes in the transfer function and adds more delay to the output. The circuit was measured to have P_{1dB} of $-5.5dB$, $IIP2$ of $5.5dBm$ and $IIP3$ of $2dBm$, at $4\,GHz$. Although the $IIP3$ is ideally 9.6dB higher than P_{1dB}, this value could be lower in reality, which is $7.5dB$ in this work. The difference could come from the mixing of fundamental and second harmonic and measurement uncertainty. The microphotograph of the fabricated allpass filter is shown in Fig. 6 and occupies an area of $380\,\mu m \times 165\,\mu m$. The circuit consumed $18.5mW$ from a $1.5V$ supply.

A. Noise Analysis

When used as delay blocks in beamforming filters, the all-pass filter noise performance may limit the sensitivity of the beamformer. Therefore, understanding the noise contributions in the filter is important for proper design trade-offs, and in particular noise factor. While noise factor is not necessarily the most appropriate noise performance metric, it is the most directly measurable. Assuming that the gate noise is negligible and $g_m >> g_{ds}$, the noise factor of Fig. 2 at low frequency can be shown to be given by (14) where noise mean-square currents $\overline{i_{M1}^2}$ and $\overline{i_{CS}^2}$ are from M_1 and PMOS current source I_B, respectively, k is Boltzmann's constant, B is the noise measurement bandwidth, and $T_0 = 290$K. A plot of the measured versus post-layout and pre-layout simulated noise figure (NF) of the allpass filter is shown in Fig. 7. Here close agreement between the measured and simulated results with the exception of the theoretical result can be seen. Note that the theoretical result in Fig. 7 includes all frequency dependent terms, whereas (14) is an approximation, which gives useful and trackable design insights.

B. Discussion

Table I compares the proposed second-order allpass filter with previously proposed wide-band allpass filters. In this table, DBW(10%) is the product of the group delay at DC and the bandwidth at which the $\tau_g(\omega)$ variation reaches 10% of its DC value [23], [27]. It can be seen that the area of the filter is lower than that of other implementations with the exception of the filter in [12] where no inductors were used. While using an inductor in the proposed allpass filter increases the filter area over other implementations such as in [23], it can be observed that the filter achieves the highest delay-bandwidth product among the second-order allpass filters in Table I.

V. CONCLUSION

In this work, a novel second order allpass filter derived from a bandpass filter is proposed. The circuit is simple and can be easily employed where fixed delays are needed and no orthogonal tuning is required. This circuit represents one of several single transistor allpass filters that can be derived from the work of [22]. The filter can also function as a first order allpass filter when $R_2 = \infty$, but since this was not the subject of this paper it simply represents an added bonus capability of this filter. The second order allpass filter was fabricated in $0.13\mu m$ CMOS and experimental and simulation results confirm the expected theory. The circuit achieved a group delay of 55 ps across a 6 GHz bandwidth, while consuming 18.5 mW power. To the best of the authors' knowledge, the filter achieves the highest DBWs among CMOS second order allpass filters reported to date in the literature.

REFERENCES

[1] R. Schaumann and M. V. Valkenburg, *Design of analog filters*. Oxford University Press, 1 ed., 2001.

[2] D. Comer, D. Comer, and J. Gonzalez, "A high-frequency integrable bandpass filter configuration," *IEEE Transactions on Circuits and Systems II: Analog and Digital Signal Processing*, vol. 44, pp. 856 –861, October 1997.

[3] S. Gift, "The application of all-pass filters in the design of multiphase sinusoidal systems," *Microelectronics Journal (Elsevier)*, vol. 31, pp. 9 – 13, January 2000.

[4] W. Tangsrirat, T. Dumawipata, and W. Surakampontorn, "Multiple-input single-output current-mode multifunction filter using current differencing transconductance amplifiers," *AEU - International Journal of Electronics and Communications (Elsevier)*, vol. 61, pp. 209 – 214, April 2007.

[5] L. Wei and I. Korn, "Combined frequency and differential phase shift keying with non-coherent detection in a satellite mobile channel," *IEEE Transactions on Vehicular Technology*, vol. 44, pp. 603 – 612, August 1995.

[6] A. Ulusoy, B. Schleicher, and H. Schumacher, "A tunable differential all-pass filter for UWB true time delay and phase shift applications," *IEEE Microwave and Wireless Components Letters*, vol. 21, pp. 462 –464, September 2011.

[7] A. Madanayake, L. Belostotski, C. Wijenayake, and L. Bruton, "Analog 2D fan filters from discrete domain transfer functions," in *IEEE International Symposium on Circuits and Systems*, (Rio De Janeiro), pp. 1652 – 1655, 15-18 May 2011.

$$F \approx 1 + \frac{R_s}{R_{sig}} \frac{|R_{sig}L_3C_1s^2+(R_2R_{sig}C_1+L_3(1+g_mR_2))s+R_{sig}(1+g_mR_2)|^2}{|R_sL_3C_1s^2+R_2(R_sC_1-g_mL_3)s+R_2+R_s(1+g_mR_2)|^2} \left(1+\frac{R_s\overline{i_{CS}^2}}{4kT_0B}\right) + \frac{R_2^2}{4kT_0BR_{sig}} \frac{|L_3C_1(R_s+R_{sig})s^2+L_3s+R_{sig}|^2}{|R_sL_3C_1s^2+R_2(R_sC_1-g_mL_3)s+R_2+R_s(1+g_mR_2)|^2}\overline{i_{M1}^2} \quad (14)$$

Table I
SUMMARY OF PUBLISHED WIDE-BAND ALLPASS FILTERS.

Ref.	Mode	Order	Output	Delay	Pole/zero freq.	Technology	# of L	P_{1dB} dBm	Area (mm^2)	DBW (10%)	Power (mW)
[6]	Volt.	2nd	Diff.	75 ps	10 GHz	SiGeRF HBT	2	-1	0.4197	0.525	38.8
[23]	Volt.	2nd	Diff.	49 ps	4.38 GHz	180 nm CMOS	0	-3.75	0.0512	0.151	16.79
[24]	Volt.	2nd	Diff.	29 ps	6.5 GHz	90 nm CMOS	0	-	-	0.081	-
[25]	Volt.	2nd	Single	84 ps	4 GHz	250 nm CMOS	0	-	0.085	0.067	30
[26]	Volt.	-	Single	50 ps	8 GHz**	SiGe BiCMOS	1	-	0.49*	0.15	121
[13]	Curr.	2nd	Single	58 ps	10 GHz	130 nm CMOS	1	-1.5	-	0.464	16.5
This work	Volt.	2nd	Single	55 ps	6 GHz	130 nm CMOS	1	-5.5	0.0627	0.55	18.5

*The total circuit area, including probe pads.
**DBW (10%) is not stated in the paper and since the group delay varies by 40% in band, DBW(10%) is not specified.

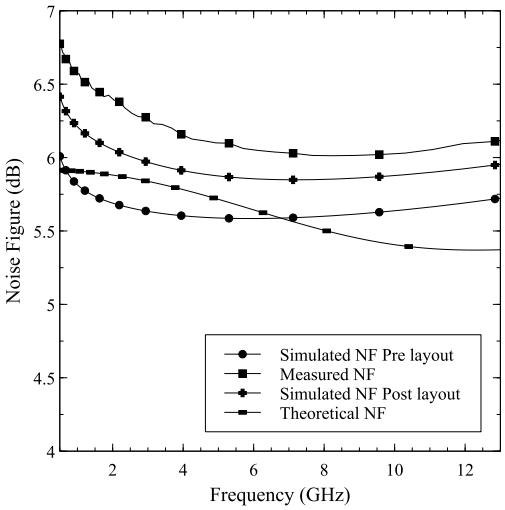

Figure 7. Plot of the measured NF, simulated pre- and post layout noise figures, and the theoretical NF of the proposed allpass filter with frequency.

[8] C. Wijenayake, Y. Xu, A. Madanayake, L. Belostotski, and L. Bruton, "RF analog beamforming fan filters using CMOS all-pass time delay approximations," *IEEE Transactions on Circuits and Systems I: Regular Papers*, vol. 59, pp. 1061 – 1073, May 2012.

[9] P. Ahmadi, M. Taghavi, L. Belostotski, and A. Madanayake, "6-GHz all-pass-filter-based delay-and-sum beamformer in 130nm CMOS," in *IEEE International Midwest Symposium on Circuits and Systems*, (College Station, USA), pp. 837–840, 3-6 August 2014.

[10] J. Schwartz, I. Arnedo, M. Laso, T. Lopetegi, J. Azana, and D. Plant, "An electronic UWB continuously tunable time-delay system with nanosecond delays," *IEEE Microwave and Wireless Components Letters*, vol. 18, pp. 103 –105, February 2008.

[11] H. Wu, J. Tierno, P. Pepeljugoski, J. Schaub, S. Gowda, J. Kash, and A. Hajimiri, "Differential 4-tap and 7-tap transverse filters in SiGe for 10Gb/s multimode fiber optic link equalization," in *IEEE International Solid-State Circuits Conference*, (San Francisco), pp. 180 – 486, 9-13 February 2003.

[12] J. Buckwalter and A. Hajimiri, "An active analog delay and the delay reference loop," in *IEEE Radio Frequency Integrated Circuits Symposium*, (Fort Worth), pp. 17 – 20, 6-8 June 2004.

[13] P. Ahmadi, M. Taghavi, L. Belostotski, and A. Madanayake, "10 GHz current-mode 1st and 2nd-order allpass filters on 130nm CMOS," in *IEEE International Midwest Symposium on Circuits and Systems*, (Columbus), pp. 1–4, 5-7 August 2013.

[14] S.-T. Liu and J.-L. Lee, "Insensitive current/voltage-mode filters using FTFNs," *Electronics Letters*, vol. 32, pp. 1079 – 1080, June 1996.

[15] O. Cicekoglu, H. Kuntman, and S. Berk, "All-pass filters using a single current conveyor," *International Journal of Electronics*, vol. 86, pp. 947–955, August 1999.

[16] J.-W. Horng, "High-input impedance voltage-mode universal biquadratic filter using three plus-type CCIIs," *IEEE Transactions on Circuits and Systems II: Analog and Digital Signal Processing*, vol. 48, pp. 996 – 997, October 2001.

[17] N. Herencsar, S. Minaei, J. Koton, E. Yuce, and K. Vrba, "New resistorless and electronically tunable realization of dual-output VM all-pass filter using VDIBA," *Analog Integrated Circuits and Signal Processing (Springer)*, vol. 74, pp. 141 – 154, January 2013.

[18] A. Toker and S. Ozoguz, "Tunable allpass filter for low voltage operation," *Electronics Letters*, vol. 39, pp. 175 – 176, January 2003.

[19] A. Toker, S. Ozoguz, O. Cicekoglu, and C. Acar, "Current-mode all-pass filters using current differencing buffered amplifier and a new high-Q bandpass filter configuration," *IEEE Transactions on Circuits and Systems II: Analog and Digital Signal Processing*, vol. 47, pp. 949 – 954, September 2000.

[20] A. Elwakil and B. Maundy, "On the two-port network analysis of common amplifier topologies," *International Journal of Circuit Theory and Applications*, vol. 38, no. 10, pp. 1087 – 1100, 2010.

[21] P. Ahmadi, M. Taghavi, L. Belostotski, and A. Madanayake, "A 0.13um CMOS current-mode all-pass filter for multi-GHz operation," *IEEE Transactions on Very Large Scale Integration (VLSI) Systems*, no. 99, 2015.

[22] A. S. Elwakil and B. J. Maundy, "Single transistor active filters: What is possible and what is not," *IEEE Transactions on Circuits and Systems I: Regular Papers*, vol. 61, no. 9, pp. 2517 – 2524, 2014.

[23] Y.-W. Chang, T.-C. Yan, and C.-N. Kuo, "Wideband time-delay circuit," in *European Microwave Integrated Circuits Conference (EuMIC)*, (Manchester), pp. 454 – 457, 9-14 October 2011.

[24] M. Maeng, F. Bien, Y. Hur, H. Kim, S. Chandramouli, E. Gebara, and J. Laskar, "0.18-μm CMOS equalization techniques for 10-Gb/s fiber optical communication links," *IEEE Transactions on Microwave Theory and Techniques*, vol. 53, no. 11, pp. 3509–3519, 2005.

[25] X. Lin, J. Liu, H. Lee, and H. Liu, "A 2.5- to 3.5-Gb/s adaptive FIR equalizer with continuous-time wide-bandwidth delay line in 0.25-μm CMOS," *IEEE Journal of Solid-State Circuits*, vol. 41, pp. 1908–1918, Aug 2006.

[26] M. Hamouda, G. Fischer, R. Weigel, and T. Ussmueller, "A compact analog active time delay line using SiGe BiCMOS technology," in *IEEE International Symposium on Circuits and Systems*, (Beijin), pp. 1055 – 1058, 19-23 May 2013.

[27] L. Zhou, A. Safarian, and P. Heydari, "CMOS wideband analogue delay stage," *Electronics Letters*, vol. 42, pp. 1213 – 1214, October 2006.